Damping of Josephson Oscillations in Strongly Correlated One-Dimensional Atomic Gases

J. Polo,[1] V. Ahufinger,[2] F. W. J. Hekking,[1,*] and A. Minguzzi[1]
[1]*Univ. Grenoble Alpes, CNRS, LPMMC, F-38000 Grenoble, France*
[2]*Departament de Física, Universitat Autònoma de Barcelona, E-08193 Bellaterra, Spain*

(Received 19 December 2017; published 31 August 2018)

We study Josephson oscillations of two strongly correlated one-dimensional bosonic clouds separated by a localized barrier. Using a quantum-Langevin approach and the exact Tonks-Girardeau solution in the impenetrable-boson limit, we determine the dynamical evolution of the particle-number imbalance, displaying an effective damping of the Josephson oscillations which depends on barrier height, interaction strength, and temperature. We show that the damping originates from the quantum and thermal fluctuations intrinsically present in the strongly correlated gas. Because of the density-phase duality of the model, the same results apply to particle-current oscillations in a one-dimensional ring where a weak barrier couples different angular momentum states.

DOI: 10.1103/PhysRevLett.121.090404

The Josephson effect was discovered in 1962 [1] when analyzing the dynamics of two superconductors coupled by a thin layer of insulating material. It is one of the most clear manifestations of macroscopic quantum coherence: its dynamical behavior, based on quantum tunneling, is fixed by the relative phase between the superconductors and has played a crucial role in the development of technological applications of superconductor materials [2].

In ultracold atomic gases, the Josephson effect has been predicted [3,4] and experimentally observed in Bose–Einstein condensates trapped in a double-well potential (external Josephson effect [5–7]) or belonging to two, Raman-coupled, internal states (internal Josephson effect [8,9]). Josephson oscillations were also observed in paired atomic Fermi gases [10,11]. In Bose-Josephson junctions, the interplay between tunneling and repulsive interactions gives rise to various dynamical regimes [4,12,13], such as Rabi [14] and Josephson [5,15,16] oscillations as well as macroscopic quantum self-trapping [4,5]. Weakly coupled Bose gases are key elements in the development of quantum technologies based on ultracold atoms, e.g., matter-wave interferometers [15,17] and sensors [18], as well as quantum computers [19,20] and atomtronics devices [21–23].

The theoretical description of Bose-Josephson junctions is generally based on a two-mode model: at mean field level, a two-mode Gross-Pitaevskii equation predicts Josephson oscillations as well as macroscopic quantum self-trapping [4,12,13]. A quantum description based on the two-mode Bose-Hubbard model allows us to capture squeezing [24,25], quantum self-trapping [26], and the formation of macroscopic superposition states [27]. Theories beyond the two-mode model show that the latter may provide inaccurate values for the Josephson-plasma frequency [28], overestimate the coherence [29] as well as the self-trapping effect [30–32], and report collapse and revivals of Josephson oscillations [33].

The Josephson effect becomes particularly intriguing when the quantum character of the Bose gas emerges, beyond the two-mode model description. Low dimensional systems provide an ideal geometry to study the quantum behavior of Bose-Josephson junctions, since quantum fluctuations and correlation effects are enhanced. The strongly correlated regime for atomic gases trapped in quasi-one-dimensional waveguides has been reached [34,35] and largely studied experimentally [34,36–40].

In the present work, we focus on the Josephson dynamics among two strongly correlated one-dimensional bosonic systems coupled head-to-tail through a weak link, as depicted in Fig. 1(a). This geometry is complementary to the one of Refs. [36,40,41], where two parallel one-dimensional wires were considered, and damped Josephson oscillations [40] were observed. In the present case, atom tunnelling between the two wires occurs only through a very small region of both clouds, and using the Luttinger-liquid (LL) effective theory, we show that the remaining part of the elongated clouds act as effective baths due to their low-energy phononlike excitations and provides an effective damping of the Josephson oscillations. An exact solution in the fermionized Tonks-Girardeau limit allows us then to obtain the full dynamical behavior following a quench in the external potential, thus offering an insight on the type of excitations contributing to the oscillations and their damping.

Exploiting the duality of the Luttinger-liquid model, our theoretical framework allows us also to describe bosons in a one-dimensional ring with a weak barrier under a gauge field, e.g., due to barrier stirring, in which we predict damping in the current oscillations following an initial

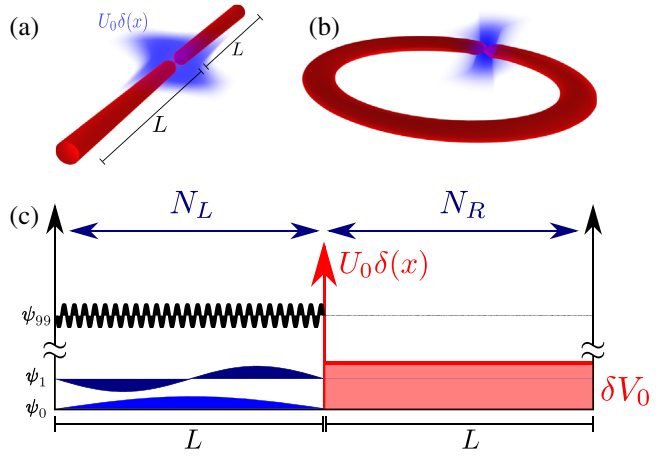

FIG. 1. Scheme of the geometries considered in this work: two weakly coupled atomic waveguides (a) and a ring potential split by a weak barrier (b). (c) Single-particle wave functions $\psi_j(x)$ used as initial condition in the TG solution and the corresponding confining potential.

quench. Experimental progresses towards the realization of such a system have been reported [42–49], although the one-dimensional regime has not yet been reached.

We start by considering two tunnel-coupled, strongly interacting, one-dimensional bosonic fluids, each confined within a tight waveguide of length L. To describe the system at intermediate and large interactions, we use the Luttinger-liquid low-energy theory, corresponding to a quantum hydrodynamic theory for density and phase fluctuations (see, e.g., [50]). The total Hamiltonian is given by two Luttinger liquids, $\hat{H}_{\mathrm{LL}\pm}$, with $+$ and $-$ for the right and left waveguides, respectively, coupled by a tunnel term, yielding a special limit of a boundary sine-Gordon model (see [51] and Refs. therein):

$$\hat{H}_{\mathrm{LL}\pm} = \frac{\hbar v_\pm K_\pm}{2\pi}\int_0^L dx\left([\partial_x\hat{\varphi}_\pm(x)]^2 + \frac{1}{K_\pm^2}[\partial_x\hat{\theta}_\pm(x)]^2\right) \tag{1}$$

$$\hat{H}_t = -E_J\cos[\hat{\varphi}_+(0^+) - \hat{\varphi}_-(0^-)], \tag{2}$$

where $\partial_x\hat{\theta}_\pm(x)/\pi$ is the density-fluctuation field operator, conjugate to the phase operator $\hat{\varphi}_\pm(x)$, fulfilling $[\partial_x\hat{\theta}_\pm(x)/\pi, \hat{\varphi}_\pm(x')] = -i\delta(x-x')$ [52]. The LL Hamiltonians (1) are expressed in terms of two parameters, the velocities $v_\pm$ of the low-energy excitations and the dimensionless Luttinger parameters $K_\pm$, related to the compressibility of each cloud [50]. In the following, we assume for simplicity that the two atomic waveguides are identical and set $v_+ = v_- = v$ and $K_+ = K_- = K$. The tunnel Hamiltonian $\hat{H}_t$ describes the presence of a large, localized barrier whose microscopic parameters determine the Josephson energy E_J (see, e.g., [53]).

We proceed by representing the Hamiltonians (1) and (2) on the normal modes basis of each Luttinger liquid, namely, the zero modes $\hat{N}_\pm$, counting the particle number in each waveguide and their conjugates phases $\hat{\phi}_{0\pm}$, as well as the position $\hat{Q}_{\mu\pm}$ and momentum $\hat{P}_{\mu\pm}$ operators for each excitation with wave vector $k_\mu = \pi\mu/L$ and frequency $\Omega_\mu = vk_\mu$. We then focus on the relative-variable problem, which is nonquadratic due to the tunnel barrier term (2), and we introduce $\hat{N} \equiv \frac{1}{2}(\hat{N}_+ - \hat{N}_-)$, $\hat{\phi}_0 \equiv \hat{\phi}_{0+} - \hat{\phi}_{0-}$ for the zero modes and $\hat{Q}_\mu \equiv \hat{Q}_{\mu+} - \hat{Q}_{\mu-}$ and $\hat{P}_\mu \equiv \frac{1}{2}(\hat{P}_{\mu+} - \hat{P}_{\mu-})$ for the excited modes. The resulting Hamiltonian reads (see the Supplemental Material [54])

$$\hat{H}_T^{\mathrm{rel}} = \frac{\hbar^2}{2ML^2}(\hat{N} - N_{\mathrm{ex}})^2 - E_J\cos(\hat{\phi}_0) + \sum_{\mu\geq 1}\left[\frac{1}{2M}\left(\hat{P}_\mu + \frac{\sqrt{2}\hbar}{L}(\hat{N} - N_{\mathrm{ex}})\right)^2 + \frac{1}{2}M\Omega_\mu^2\hat{Q}_\mu^2\right], \tag{3}$$

with effective mass $M = \hbar K/2\pi vL = K^2 m/2\pi^2 N_0$, N_0 the average particle number in each tube, and $N_{\mathrm{ex}} \ll N_0$ the excitation imbalance, which may be tuned by a suitable choice of the initial conditions. We identify in Eq. (3) a quantum particle term corresponding to the two collective variables $\hat{N}$ and $\hat{\phi}_0$, a bath of harmonic oscillators formed by the excited modes, and a coupling term $\propto \hat{P}_\mu\hat{N}$, obtained by expanding the second line of Eq. (3). The same structure is found in the Caldeira-Leggett Hamiltonian [55–57]; however, in our model, the bath of harmonic oscillators is intrinsic in the model, originated from the phonon excitations in the Bose fluid, while in the Caldeira-Leggett model it is phenomenologically introduced. The first line of Eq. (3) corresponds to the familiar Josephson Hamiltonian, where two regimes are possible depending on the ratio of the Josephson E_J and kinetic $E_Q = \hbar^2/ML^2 = 2\Delta E/K$ energies, with $\Delta E = \hbar\pi v/L$ being the level spacing among phonon modes of the bath. Notice that E_J and E_Q depend on interactions, since the tunnel energy is renormalized by quantum fluctuations [58], and both the sound velocity and the Luttinger parameter vary with interaction strength [50].

We start from the case $E_J \gg E_Q$, where the Josephson potential term $-E_J\cos(\hat{\phi}_0)$ dominates upon the kinetic energy. Starting from an initial particle imbalance among the two wires, its dynamical evolution is readily obtained from the Heisenberg equations of motion and takes a quantum Langevin form:

$$\ddot{\hat{N}} + \omega_0^2\cos(\hat{\phi}_0)\hat{N} + \int_0^t dt'\gamma_N(t,t')\dot{\hat{N}}(t') = \xi_N(t), \tag{4}$$

with (see the Supplemental Material [54]) $\omega_0 = \sqrt{E_J E_Q}/\hbar$ the Josephson frequency, $\gamma_N(t,t')$ the memory-friction

kernel, and $\xi_N(t)$ the quantum noise generated by the phonon bath. $\gamma_N(t,t')$ can be approximated to be local in time in the case of long wires, where many excited phonons contribute to the bath, and in the low-energy regime, where the high-energy cutoff of the LL theory is the largest energy scale in the problem. In the high-temperature, regime we have $\langle\xi_N(t)\rangle = 0$ and $\langle\xi_N(t)\xi_N(t')\rangle = \eta\delta(t-t')$, with $\eta = 2E_J^2 k_B T/\hbar^2 MLv$.

For small phase oscillations, the average relative number $N_{\rm LL} = \langle\hat{N}\rangle$ in Eq. (4) is then described by a damped harmonic oscillator with frequency $\omega_J = \sqrt{\omega_0^2 - \gamma^2}$ and damping rate $\gamma = \pi E_J/\hbar K$ [54]. In the weakly interacting limit, where $K \sim 1/\sqrt{g_{1D}}$ and $v_s \sim \sqrt{g_{1D}}$ with g_{1D} the 1D interaction strength, we recover the predictions of the two-mode model in its small-oscillation limit; i.e., we find $E_Q \propto g_{1D}$ and γ/E_Q vanishing for $g_{1D} \to 0$, yielding undamped Josephson oscillations. At increasing interactions, E_Q increases, being related to the compressibility of the system, and E_J decreases, since it is renormalized by larger and larger phase fluctuations. Since $\gamma_Q \equiv \gamma/\omega_0 = \pi\sqrt{E_J}/\sqrt{E_Q}K$, we predict that Josephson oscillations will be more and more damped at increasing interactions. Hence, quite interestingly, while remaining in the regime $E_J \gg E_Q$, both the underdamped and the overdamped Josephson oscillations can be accessed. Using realistic experimental values [36,37], i.e., $E_J/\hbar = 2\pi \times 80,\ 200,\ 900$ Hz, $L \approx 6.8\ \mu$m, $v \approx 6.7$ mm/s, and a 1D interaction strength $g_{1D}/\hbar = 0.84$ mm/s which leads to $E_Q/\hbar \approx 245$ Hz for $N = 20$, we estimate $\omega_0 \approx 2\pi \times (50-160)$ Hz and $\gamma \approx 0.4$–$20\ \omega_0$. Notice also that at fixed interactions one may explore the crossover from underdamped to overdamped oscillations by tuning the barrier strength.

In Fig. 2, we show the damped Josephson oscillations of the relative number between the two clouds, at varying barrier and interaction strength. The noise in Eq. (4) yields stochastic fluctuations in the dynamics [54], indicated as shaded areas in the figure. At long times $t \gg 1/\gamma$

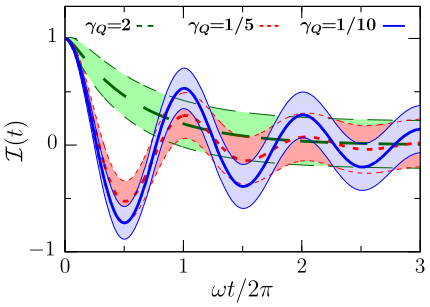

FIG. 2. Dynamics of imbalance $\mathcal{I}(t)$ (dimensionless) for relative number $N(t)/N(0)$ in tunnel-coupled wires or for current oscillations $J(t)/J(0)$ in a ring, from the LL approach, for various values of $\gamma_Q = \gamma/\omega_0$ or $\gamma_Q = \gamma^{\rm r}/\omega_0^{\rm r}$, respectively. The corresponding uncertainties due to the stochastic noise are indicated in the shaded areas.

and in the high-temperature regime, we have $\Delta N_{\rm LL} = \langle(\hat{N} - \langle\hat{N}\rangle)^2\rangle^{1/2} = \sqrt{(ML^2/\hbar^2)k_B T}$, which coincides with the high-temperature limit found using the fluctuation dissipation theorem [54,59]. Of course, in any closed, finite, quantum system revivals are expected and would occur if a discrete phonon spectrum is used. In a semiclassical approach, for example, revivals can be viewed as a resynchronization of the bath modes [60].

In the opposite regime $E_J \ll E_Q$, the phase is only weakly pinned and displays large fluctuations. The dynamics are most suitably described in the Fock basis for the relative number. The energy levels of the quantum particle seen in Eq. (3) can be described as a function of the number of excitations $N_{\rm ex}$, which plays the role of quasimomentum in crystals, and takes the form of a sequence of parabolas $\epsilon_n(N_{\rm ex}) = E_Q(n - N_{\rm ex})^2/2$, with $\hat{N}|n\rangle = n|n\rangle$, with gaps of amplitude E_J opening at semi-integer values of $N_{\rm ex}$. Close to the anticrossing points $N_{\rm ex} = \pm 1/2, \pm 3/2, \ldots$, the system behaves as an effective two-level model. In this case, the Josephson dynamics correspond to the Rabi oscillations of the quantum particle, with frequency $E_J/\hbar$. Because of the large value of E_Q, which also fixes the scale of bath modes-level spacing, in this regime, there is no effect of the bath modes on the quantum particle.

The Luttinger liquid model is very useful because it allows us to describe a large range of interaction strengths, though it remains an effective model. In the following, we take a complementary approach and solve the exact quantum mechanical evolution in the limit of infinitely strong repulsive interactions, i.e., the Tonks-Girardeau (TG) regime [61], corresponding to the case $K = 1$ of the LL theory. In this limit, using the time-dependent Bose-Fermi mapping [61–63], the many-body wave function Ψ_{TG} can be written as

$$\Psi_{\rm TG}(x_1,\ldots,x_N) = \Pi_{1\le j\le \ell\le N}\,\mathrm{sgn}(x_j - x_\ell)\,\det[\psi_k(x_j,t)], \quad (5)$$

where $\psi_j(x,t)$ is the solution of the single-particle Schrödinger equation $i\hbar\partial_t\psi_j = (-\hbar^2\partial_x^2/2m + V(x,t))\psi_j$ with initial conditions $\psi_j(x,0) = \psi_j$ being the eigenfunctions of the Schrödinger problem at the initial time. To induce Josephson oscillations, we perform a quench in the confining potential $V(x,t)$ [64,65], taken as a box potential separated in two parts by a delta barrier $U_0\delta(x)$ with an imbalance δV_0 between left and right waveguides at the initial time [see Fig. 1(c)]. δV_0 is then set to zero during the time evolution, inducing $2N_{\rm ex}$ excitations above the Fermi energy. The total density profile of the TG gas at finite temperature is $n(x,t) = \sum_{j=0}^{\infty} f(\epsilon_j)|\psi_j(x,t)|^2$ [66,67], with $f(\epsilon_n)$ the Fermi-Dirac distribution and ϵ_n the nth single-particle eigenenergy, allowing us to obtain the relative particle number $N(t) = N_L - N_R$, with $N_L = \int_{-L}^{0} dx n(x,t)$ and $N_R = \int_0^L dx n(x,t)$.

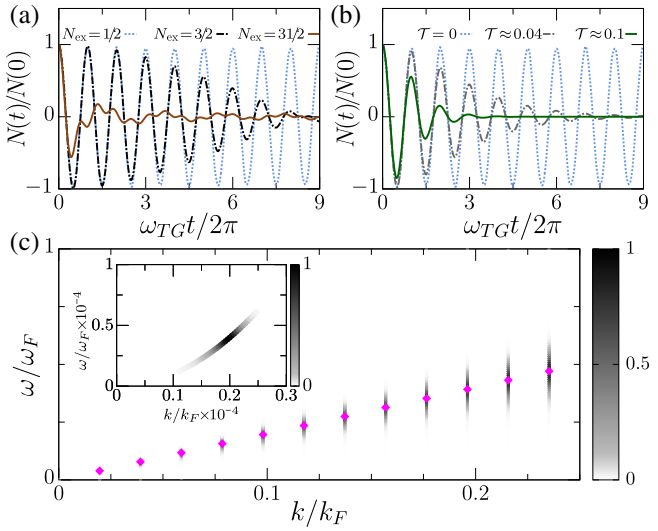

FIG. 3. Relative-number oscillations in the TG regime following a quench of the initial step potential δV_0: (a) at zero temperature for $\delta V_0/E_F = 0.07$ (blue dotted line), 0.14 (black dashed line), and 0.72 (brown solid line), with E_F the Fermi energy and (b) at finite temperature for $\delta V_0/E_F = 0.07$. (c) Exact TG excitation spectrum (dimensionless, gray-scale points) in the frequency-wave vector plane for $T/T_F = 0.1$ and LL excitation spectrum (magenta points). Inset: zoom on the small-k region. In all panels, $N_T = 101$ and $\lambda \equiv 2mLU_0/\hbar^2\pi^2 N_T = 200$.

In Fig. 3(a), we show the exact dynamics of $N(t)$ following the quench in the step potential. We observe that for an initial small imbalance, corresponding to $N_{\rm ex} = 1/2$, undamped oscillations occur, with frequency $\omega_{\rm TG} = \epsilon_{N+1} - \epsilon_N$. For a larger imbalance, an effective damping appears, as a consequence of the several frequencies associated to the excitations involved in the dynamics. The exact solution allows us also to address the long-time dynamics where oscillations display revivals [54] since the system has finite size. In order to make connection with the LL model, we notice that for bosons in the TG regime $E_J = \hbar\omega_{\rm TG}$ and $E_Q = \hbar^2\pi^2 N/mL^2$. For the parameters used in Fig. 3, $E_J/E_Q = 4\times10^{-3}$. Hence, the oscillations observed in the exact solutions at small δV_0 are the undamped Rabi oscillations of the quantum particle predicted by the LL model. For larger imbalance, the exact dynamics corresponds to large-amplitude oscillations, beyond the LL treatment.

Figure 3(b) shows the small-imbalance dynamics at finite temperature. At differences from the predictions of the LL model, we find damped oscillations. In order to pinpoint the origin of this damping, using the exact solution, we calculate the spectral function [54] for the system at finite temperature, see Fig. 3(c). While the exact spectral function contains multiple particle-hole excitations, the LL model assumes a linear excitation spectrum. This is an excellent approximation at low energy and, in particular, for the energy scales involved in the dynamics of the current study. The exact spectral function contains also several low-energy excitations with frequencies of order E_J [inset of Fig. 3(c)], which are associated to the presence of a finite barrier and give rise to the observed damping. These modes are absent in the infinite-barrier case corresponding to the LL Hamiltonian (1). As a main conclusion of this analysis, the exact solution validates the frequency of the Josephson oscillations predicted in the LL model and the fact that oscillations may be damped by an intrinsic bath made of low-energy excitations.

The Luttinger-liquid analysis applies also to a dual system made of ultracold bosons confined in a ring trap of circumference length L, containing a small, localized barrier and subjected to an artificial gauge field Ω. In this system, we follow the dynamical evolution of the average current as a function of time, following a sudden quench of Ω. This can be induced, for instance, by transferring orbital angular momentum on the atoms with a Laguerre-Gauss beam [68] by phase imprinting [69], by stirring a potential barrier [70], or by modulating an artificial gauge field [71]. We model the system by a single LL Hamiltonian that describes the particles in the ring,

$$\hat{H}_{\rm LL} = \frac{\hbar v K}{2\pi}\int_0^L dx\left(\left[\partial_x\hat{\varphi}(x) - \frac{2\pi}{L}\Omega\right]^2 + \frac{1}{K^2}[\partial_x\hat{\theta}(x)]^2\right), \tag{6}$$

plus a weak delta potential barrier $U(x) = U_0\delta(x)$, with corresponding Hamiltonian $\hat{H}_b = 2n_0U_{\rm eff}\cos[2\hat{\theta}(x=0)]$, with $n_0 = N_T/L$ and $U_{\rm eff}$ the effective barrier strength [58]. Notice that the duality of the model follows from the density-phase duality of the LL Hamiltonian as well as the duality between strong- and weak-barrier limits in the LL description. In the ring geometry, the relevant collective variables are the current and zero-mode density field operator, fulfilling $[\hat{\theta}_0, \hat{J}] = i/2$. By following a procedure similar to the coupled waveguide case [54,72], we find the effective Hamiltonian:

$$\hat{H}_T = \frac{\hbar^2(2\pi)^2}{2M_{\rm r}L^2}(\hat{J}-\Omega)^2 - 2n_0U_{\rm eff}\cos(2\hat{\theta}_0) + \sum_{\mu\geq1}\left[\frac{1}{2M_{\rm r}}\left(\hat{P}_\mu + \frac{4\pi\sqrt{2}\hbar}{L}(\hat{J}-\Omega)\right)^2 + \frac{1}{2}M_{\rm r}\Omega_\mu^2\hat{Q}_\mu^2\right], \tag{7}$$

where the quantum particle is now the current, $M_{\rm r} = (\hbar\pi/vLK)$ and $\Omega_\mu = vk_\mu$ are the mass and frequencies of the bath modes, and in this case, $E_Q^{\rm r} = \hbar^2(2\pi)^2/M_{\rm r}L^2$ and $E_J^{\rm r} = 2n_0U_{\rm eff}$. When $E_J^{\rm r} > E_Q^{\rm r}$, the small oscillations of the current (see Fig. 2) are again described by a harmonic oscillator with frequency $\omega_0^{\rm r} = \sqrt{E_Q^{\rm r}E_J^{\rm r}}/\hbar$ and damping rate $\gamma^{\rm r} = 4\pi E_J^{\rm r}K/\hbar$. The effective damping originates from

the phonon modes of the ring. Notice that in this dual model damping decreases at increasing interactions. In the opposite regime $E_J^r < E_Q^r$, for small imbalances we expect undamped Rabi oscillations among angular momentum states. The exact TG solution for a quantum quench of the artificial gauge field on a ring shows weakly damped oscillations and the formation of nonclassical states [65].

In conclusion, by combining Luttinger-liquid theory and an exact solution at infinite interactions, we have studied the Josephson oscillations of particle imbalance among two atomic waveguides as well as particle-current oscillations along a ring. In both cases, we have found that an intrinsic damping is present in the oscillations due to the coupling with the collective excitations in the system. Our approach also yields analytical expressions for the natural frequencies and damping rates as a function of the microscopic parameters of the model. In a similar fashion, the bath phonon modes gives rise to damping of current-current time correlation functions [74]. Our results are relevant not only to ongoing studies on the bosonic Josephson effect at different interactions strengths but also to future developments of quantum devices in which dissipation and thermalization can be limiting factors to perform quantum computations. Moreover, the results in ring potentials are particularly relevant to current experiments, in particular, to atomtronic devices [23,44,75] where the interplay of interactions and barrier strength is crucial when creating persistent currents.

We would like to thank R. Dubessy, M. Filippone, P. Pedri, and H. Perrin for useful discussions. The authors acknowledge financial support through the ANR project SuperRing (Grant No. ANR-15-CE30-0012-02). J. P. and V. A. acknowledge the Spanish Ministry of Economy and Competitiveness (MINECO) (Contract No. FIS2014-57460-P), and J. P. acknowledges the mobility Grant No. EEBB-I-15-10194.

[*] Deceased.

[1] B. Josephson, Phys. Lett. **1**, 251 (1962).
[2] A. Barone and G. Paternò, *Physics and Applications of the Josephson Effect* (John Wiley & Sons, New York, 1982).
[3] J. Javanainen, Phys. Rev. Lett. **57**, 3164 (1986).
[4] A. Smerzi, S. Fantoni, S. Giovanazzi, and S. R. Shenoy, Phys. Rev. Lett. **79**, 4950 (1997).
[5] M. Albiez, R. Gati, J. Fölling, S. Hunsmann, M. Cristiani, and M. K. Oberthaler, Phys. Rev. Lett. **95**, 010402 (2005).
[6] Y. Shin, G.-B. Jo, M. Saba, T. A. Pasquini, W. Ketterle, and D. E. Pritchard, Phys. Rev. Lett. **95**, 170402 (2005).
[7] S. Levy, E. Lahoud, I. Shomroni, and J. Steinhauer, Nature **449**, 579 (2007).
[8] J. Williams, R. Walser, J. Cooper, E. Cornell, and M. Holland, Phys. Rev. A **59**, R31 (1999).
[9] T. Zibold, E. Nicklas, C. Gross, and M. K. Oberthaler, Phys. Rev. Lett. **105**, 204101 (2010).
[10] G. Valtolina, A. Burchianti, A. Amico, E. Neri, K. Xhani, J. A. Seman, A. Trombettoni, A. Smerzi, M. Zaccanti, M. Inguscio, and G. Roati, Science **350**, 1505 (2015).
[11] A. Burchianti, F. Scazza, A. Amico, G. Valtolina, J. A. Seman, C. Fort, M. Zaccanti, M. Inguscio, and G. Roati, Phys. Rev. Lett. **120**, 025302 (2018).
[12] I. Zapata, F. Sols, and A. J. Leggett, Phys. Rev. A **57**, R28 (1998).
[13] S. Raghavan, A. Smerzi, S. Fantoni, and S. R. Shenoy, Phys. Rev. A **59**, 620 (1999).
[14] F. S. Cataliotti, S. Burger, C. Fort, P. Maddaloni, F. Minardi, A. Trombettoni, A. Smerzi, and M. Inguscio, Science **293**, 843 (2001).
[15] T. Schumm, S. Hofferberth, L. M. Andersson, S. Wildermuth, S. Groth, I. Bar-Joseph, J. Schmiedmayer, and P. Krüger, Nat. Phys. **1**, 57 (2005).
[16] L. J. LeBlanc, A. B. Bardon, J. McKeever, M. H. T. Extavour, D. Jervis, J. H. Thywissen, F. Piazza, and A. Smerzi, Phys. Rev. Lett. **106**, 025302 (2011).
[17] M. R. Andrews, C. G. Townsend, H.-J. Miesner, D. S. Durfee, D. M. Kurn, and W. Ketterle, Science **275**, 637 (1997).
[18] B. V. Hall, S. Whitlock, R. Anderson, P. Hannaford, and A. I. Sidorov, Phys. Rev. Lett. **98**, 030402 (2007).
[19] G.-B. Jo, Y. Shin, S. Will, T. A. Pasquini, M. Saba, W. Ketterle, D. E. Pritchard, M. Vengalattore, and M. Prentiss, Phys. Rev. Lett. **98**, 030407 (2007).
[20] J. Estève, C. Gross, A. Weller, S. Giovanazzi, and M. K. Oberthaler, Nature (London) **455**, 1216 (2008).
[21] D. Aghamalyan, L. Amico, and L. C. Kwek, Phys. Rev. A **88**, 063627 (2013).
[22] L. Amico, D. Aghamalyan, F. Auksztol, H. Crepaz, R. Dumke, and L. C. Kwek, Sci. Rep. **4**, 4298 (2014).
[23] D. Aghamalyan, M. Cominotti, M. Rizzi, D. Rossini, F. Hekking, A. Minguzzi, L.-C. Kwek, and L. Amico, New J. Phys. **17**, 045023 (2015).
[24] K. Maussang, G. E. Marti, T. Schneider, P. Treutlein, Y. Li, A. Sinatra, R. Long, J. Estève, and J. Reichel, Phys. Rev. Lett. **105**, 080403 (2010).
[25] B. Juliá-Díaz, T. Zibold, M. K. Oberthaler, M. Melé-Messeguer, J. Martorell, and A. Polls, Phys. Rev. A **86**, 023615 (2012).
[26] B. Juliá-Díaz, J. Martorell, and A. Polls, Phys. Rev. A **81**, 063625 (2010).
[27] G. Ferrini, A. Minguzzi, and F. W. J. Hekking, Phys. Rev. A **80**, 043628 (2009).
[28] A. Burchianti, C. Fort, and M. Modugno, Phys. Rev. A **95**, 023627 (2017).
[29] A. Vardi and J. R. Anglin, Phys. Rev. Lett. **86**, 568 (2001).
[30] F. Meier and W. Zwerger, Phys. Rev. A **64**, 033610 (2001).
[31] K. Sakmann, A. I. Streltsov, O. E. Alon, and L. S. Cederbaum, Phys. Rev. Lett. **103**, 220601 (2009).
[32] R. Hipolito and A. Polkovnikov, Phys. Rev. A **81**, 013621 (2010).
[33] G. J. Milburn, J. Corney, E. M. Wright, and D. F. Walls, Phys. Rev. A **55**, 4318 (1997).
[34] B. Paredes, A. Widera, V. Murg, O. Mandel, S. Fölling, I. Cirac, G. V. Shlyapnikov, T. W. Hänsch, and I. Bloch, Nature (London) **429**, 277 (2004).
[35] T. Kinoshita, T. Wenger, and D. S. Weiss, Science **305**, 1125 (2004).

[36] S. Hofferberth, I. Lesanovsky, B. Fischer, T. Schumm, and J. Schmiedmayer, Nature (London) **449**, 324 (2007).
[37] S. Hofferberth, I. Lesanovsky, T. Schumm, A. Imambekov, V. Gritsev, E. Demler, and J. Schmiedmayer, Nat. Phys. **4**, 489 (2008).
[38] E. Haller, M. Gustavsson, M. J. Mark, J. G. Danzl, R. Hart, G. Pupillo, and H.-C. Nägerl, Science **325**, 1224 (2009).
[39] B. Yang, Y.-Y. Chen, Y.-G. Zheng, H. Sun, H.-N. Dai, X.-W. Guan, Z.-S. Yuan, and J.-W. Pan, Phys. Rev. Lett. **119**, 165701 (2017).
[40] M. Pigneur, T. Berrada, M. Bonneau, T. Schumm, E. Demler, and J. Schmiedmayer, Phys. Rev. Lett. **120**, 173601 (2018).
[41] T. Langen, T. Schweigler, E. Demler, and J. Schmiedmayer, New J. Phys. **20**, 023034 (2018).
[42] A. Ramanathan, K. C. Wright, S. R. Muniz, M. Zelan, W. T. Hill, C. J. Lobb, K. Helmerson, W. D. Phillips, and G. K. Campbell, Phys. Rev. Lett. **106**, 130401 (2011).
[43] K. C. Wright, R. B. Blakestad, C. J. Lobb, W. D. Phillips, and G. K. Campbell, Phys. Rev. Lett. **110**, 025302 (2013).
[44] S. Eckel, J. G. Lee, F. Jendrzejewski, N. Murray, C. W. Clark, C. J. Lobb, W. D. Phillips, M. Edwards, and G. K. Campbell, Nature (London) **506**, 200 (2014).
[45] B. M. Garraway and H. Perrin, J. Phys. B At. Mol. Opt. Phys. **49**, 172001 (2016).
[46] H. Perrin and B. M. Garraway, Adv. At., Mol., Opt. Phys. **66**, 181 (2017).
[47] K. Henderson, C. Ryu, C. MacCormick, and M. G. Boshier, New J. Phys. **11**, 043030 (2009).
[48] C. Ryu, P. W. Blackburn, A. A. Blinova, and M. G. Boshier, Phys. Rev. Lett. **111**, 205301 (2013).
[49] A. Turpin, J. Polo, Y. V. Loiko, J. Küber, F. Schmaltz, T. K. Kalkandjiev, V. Ahufinger, G. Birkl, and J. Mompart, Opt. Express **23**, 1638 (2015).
[50] M. A. Cazalilla, J. Phys. B At. Mol. Opt. Phys. **37**, S1 (2004).
[51] P. Fendley, F. Lesage, and H. Saleur, J. Stat. Phys. **85**, 211 (1996).
[52] C. L. Kane and M. P. A. Fisher, Phys. Rev. B **46**, 15233 (1992).
[53] U. Weiss, Solid State Commun. **100**, 281 (1996).
[54] See Supplemental Material at http://link.aps.org/supplemental/10.1103/PhysRevLett.121.090404 for details.
[55] A. O. Caldeira and A. J. Leggett, Phys. Rev. Lett. **46**, 211 (1981).
[56] A. Caldeira and A. Leggett, Ann. Phys. (N.Y.) **149**, 374 (1983).
[57] G. Schön and A. Zaikin, Phys. Rep. **198**, 237 (1990).
[58] M. Cominotti, D. Rossini, M. Rizzi, F. Hekking, and A. Minguzzi, Phys. Rev. Lett. **113**, 025301 (2014).
[59] U. Weiss, *Quantum Dissipative Systems*, Series in Modern Condensed Matter Physics (World Scientific, Singapore, 2008).
[60] K. E. Nagaev and M. Büttiker, Europhys. Lett. **58**, 475 (2002).
[61] M. Girardeau, J. Math. Phys. **1**, 516 (1960).
[62] M. D. Girardeau and E. M. Wright, Phys. Rev. Lett. **84**, 5691 (2000).
[63] V. I. Yukalov and M. D. Girardeau, Laser Phys. Lett. **2**, 375 (2005).
[64] M. Cominotti, F. Hekking, and A. Minguzzi, Phys. Rev. A **92**, 033628 (2015).
[65] C. Schenke, A. Minguzzi, and F. W. J. Hekking, Phys. Rev. A **84**, 053636 (2011).
[66] K. Millard, J. Math. Phys. **10**, 7 (1969).
[67] K. K. Das, M. D. Girardeau, and E. M. Wright, Phys. Rev. Lett. **89**, 170404 (2002).
[68] C. Ryu, M. F. Andersen, P. Cladé, V. Natarajan, K. Helmerson, and W. D. Phillips, Phys. Rev. Lett. **99**, 260401 (2007).
[69] S. Moulder, S. Beattie, R. P. Smith, N. Tammuz, and Z. Hadzibabic, Phys. Rev. A **86**, 013629 (2012).
[70] N. Murray, M. Krygier, M. Edwards, K. C. Wright, G. K. Campbell, and C. W. Clark, Phys. Rev. A **88**, 053615 (2013).
[71] J. Dalibard, F. Gerbier, G. Juzeliūnas, and P. Öhberg, Rev. Mod. Phys. **83**, 1523 (2011).
[72] Note that in the weak barrier limit the barrier introduces a phase shift $\theta_B = \pi/2$ in the field operator $\hat{\theta}(x)$, as can be derived following [73].
[73] N. Didier, A. Minguzzi, and F. W. J. Hekking, Phys. Rev. A **79**, 063633 (2009).
[74] N. V. Prokof'ev and B. V. Svistunov, arXiv:1710.00721.
[75] R. A. Pepino, J. Cooper, D. Z. Anderson, and M. J. Holland, Phys. Rev. Lett. **103**, 140405 (2009).